International Research Journal of Geology and Mining (IRJGM) (2276-6618) Vol. 4(5) pp. 133-138, August, 2014
DOI: http:/dx.doi.org/10.14303/irjgm.2014.029
Available online http://www.interesjournals.org/irjgm

Full Length Research Paper

Amplitude Simulation Technique for Seismic Amplitude Scaling

[1]*Oppong I. A. and [2]Danour S. K.

[1]Department of Earth Science, University of Ghana, Legon, Accra, Ghana
[2]Department of Physics, Kwame Nkrumah University of Science and Technology (KNUST), Kumasi, Ghana
*Corresponding author email: iaoppong@ug.edu.gh

ABSTRACT

Conventional amplitude compensation methods in seismic data processing tend to equalize or flatten seismic amplitudes. They tend to destroy the subsurface characters in the seismic data. They also decrease signal resolution and quality, and therefore result into false interpretation of geological structures. In this paper, we report on amplitude compensation methods using Amplitude Simulation Technique (AST). The technique is based on the Principle of Amplitude Modulation. This Principle requires that the ratio of the change in amplitude of a signal at the receiver position, to the amplitude at the source location, cannot exceed unity. On the basis of this, if a seismic signal has amplitude modulation in excess of unity, the processed seismic signal will produce severe amplitude distortions and interference. On the other hand, if the amplitude modulation is far less than unity, the processed seismic signal will have poor contrast, and therefore would need further amplitude compensation to improve signal to noise ratio. The absolute amplitude of the edited seismic signal was computed and a scatter diagram of the amplitude variation with the reflection time was displayed. The amplitudes of the farther samples were matched with the first maximum amplitude. The process was iterated, till all the samples achieved the same amplitude. Using a generated equation from Parseval's Theorem, the percentage energy (amplitude) and power recovery of the new scaling functions were computed, and the results were displayed in order to choose the optimum scaling function (OSF) at a yielding point, for the seismic signal to preserve the signal signatures.

Keywords: Seismic, Amplitude, Simulation, Modulation, Optimum Scaling Function (OSF), Conventional, Yielding Point (YP), Parseval's Theorem, Signal, Noise.

INTRODUCTION

Seismic methods are essential to the discovery of oil and gas-bearing structures (Dobrin and Savit, 1988; Griffiths and King, 1981). With seismic methods, detail information about the prospective oil bearing structure can be obtained by the application of echo-sounding. In offshore areas, surveys are undertaken by a ship which normally tows submerged energy source, air or water gun, to produce short burst of sound energy, and a long streamer containing several hydrophones for measuring the variation of water pressure relative to the hydrostatic pressure. In Land Survey, geophones or receiver groups are connected to a recording truck by a cable which extends in one or both directions from the shot point (Telford *et al*., 1990; Henry, 1997; Kearey and Brooks, 2002).

In both offshore and onshore surveys, the total initial energy is spread over the wavefront which expands as it moves in the direction of propagation. The amount of energy per unit area decreases with increasing offset positions. The farther the detectors are from the shot location, the weaker the echo from the reflective interfaces (Palmer, 1980; Mike, 2007). The intensity of the recorded sound wave is then plotted against the two way time, and displayed as a wiggle trace called the spectra signature of the geology. In the absence of geology, the amplitude of the input seismic wavelet (source energy) will be equal to that of the reflected wavelet, a particular situation when the detector is positioned at the source position, and the recorded energy may not need any amplitude restoration (Yilmaz, 2001; Ikelle and Lasse, 2005). However, since the subsurface is not perfectly elastic, mechanical energy is not totally conserved during sound propagation. The corresponding absorption of energy is frequency dependent, and it attenuates the amplitude spectrum at the high frequency end of the wavelet (Telford *et al*., 1990; Henry, 1997; Kearey and Brooks, 2002).

Conventional methods include programmed gain (PG), root mean square (rms) gain, and instantaneous automatic (AGC) gain (Western Geophysical, 1998; Sandmeier, 2012), just to mention a few. These methods are computed in the time domain within selected time ranges (Henry, 1997; Sandmeier, 2012). The application of these scaling methods are then inverted, and applied to the seismic data in the time domain to equalize or flatten the amplitude of all the recorded samples in the trace. These methods of amplitude equalization tend to over-estimate or over-amplify small amplitude signals and remnant noise, but under-estimate large and true amplitude signals. In most cases, the true amplitude of the seismic signal is destroyed (Claerbout, 1976; Henry, 1997; Sandmeier, 2012).

During seismic acquisition, the amplitude of recorded seismic signal decreases with increase in time (t) and offset (x), while the frequency and phase of the signal are normally constant. The process of varying the amplitude and keeping the frequency and the phase constant is termed amplitude modulation (AM). The extent by which the seismic amplitude varies according to the position of the receivers is described as modulation index (m_{id}). The modulation index, m_{id} (Gupta, 2009), by definition is the ratio of the change in amplitude of a signal at the receiver position (a_r), to the amplitude at the origin or source location (a_m), and is expressed as:

$$m_{id} = \frac{a_r}{a_m} \qquad (1)$$

According to the Principle of Amplitude Modulation (Gupta, 2009), m_{id} cannot exceed unity. If for any reason the amplitude modulation is in excess of unity ($m_{id} > 1$), the processed signal will produce severe amplitude distortion and interference (noise trains). On the other hand, if the signal is modulated to a small amount, ($m_{id} < 1$), the signal amplitude will be smaller, and the processed signal energy will be very weak. Since recorded seismic waves are also signals resulted from the perturbation of the earth, the principle of amplitude modulation can also be applied to them.

MATERIALS AND METHODS

The procedure required to prepare the field seismic data for the amplitude matching technique is shown in Figure 1 below. The input SEG-Y represents the recorded field data, normally digitized at 2 ms, from all the traces of the spread at successive times in the Society of Exploration Geophysicists (SEG) format. This type of data is often called Multiplex seismic data, and needs to be de-multiplexed before the seismic data can be processed. At this point, if navigation data was taken at the time of acquisition with the intension of creating 3D seismic data, the de-multiplexed data can be merged with the navigation data, before further digitizing or the resample processing step. If the number of seismic channels is wrongly described, the seismic data will not line up in a 2D array.

After the demultiplexing step, the data can be resampled to 4 ms just to reduce the total volume of seismic data before any serious data processing is carried out. Resampling however, changes the frequency content of the data, in that, it causes frequency folding or aliasing, and if nothing is done to the data, there could be signal interference and distortions. For this reasons, the anti-aliasing filter is applied to remove the over fold seismic data (Sheriff, 1991).

At this stage, a side-by-side display of the seismic traces (shot gathers) which have the same shot coordinates can be displayed for quality control (QC). Noise attenuation serves to attenuate any large amplitude noise burst found on the shot display. The amplitude of each sample was examined, relative to the average amplitude in a zone preceding the sample. If the amplitude of a sample was found to exceed the average amplitude in the zone, it can be reduced to this average value, and the shot gather re-displayed to ensure that all corrections made were effective, and the new display looked better than the previous shot display. Once the shot display was satisfactory after any noise attenuation, the digitization step, using the continuous seismic data as the input data, can be started.

The method of digitization/sampling is indicated in Figures 2 and 3 below. Figure 2(a) indicates the acquisition geometry of the seismic signal, and Figure 2(b) indicates the matrix array of the sampled data (Frank, 1974). Figure 3 is the equivalent of the split-spread seismic method geometry, and its corresponding sampled matrix array. In both Figure 2 and Figure 3, D is the seismic detector, S is the signal, X is the offset, and SP is the shot point or source location. From the matrix element, $s_1t_{11}a_{11}$, in Figure 2, s_1 indicates first signal, t_{11} indicates the first sampled time (TWT) from the first signal, and a_{11} indicates the first sampled amplitude of the first signal. With the symbol '$s_Lt_{L2}a_{L2}$', s_L indicates the last signal, where t_{L2} indicates the second sampled time of the last signal, and a_{L2} is the second sampled amplitude of the last signal, and so on.

The geometry of the split spread seismic acquisition is geometrically different from the end spread method, as indicated above, hence the difference in the sampled matrix arrays. From Figure 3, the matrix element,

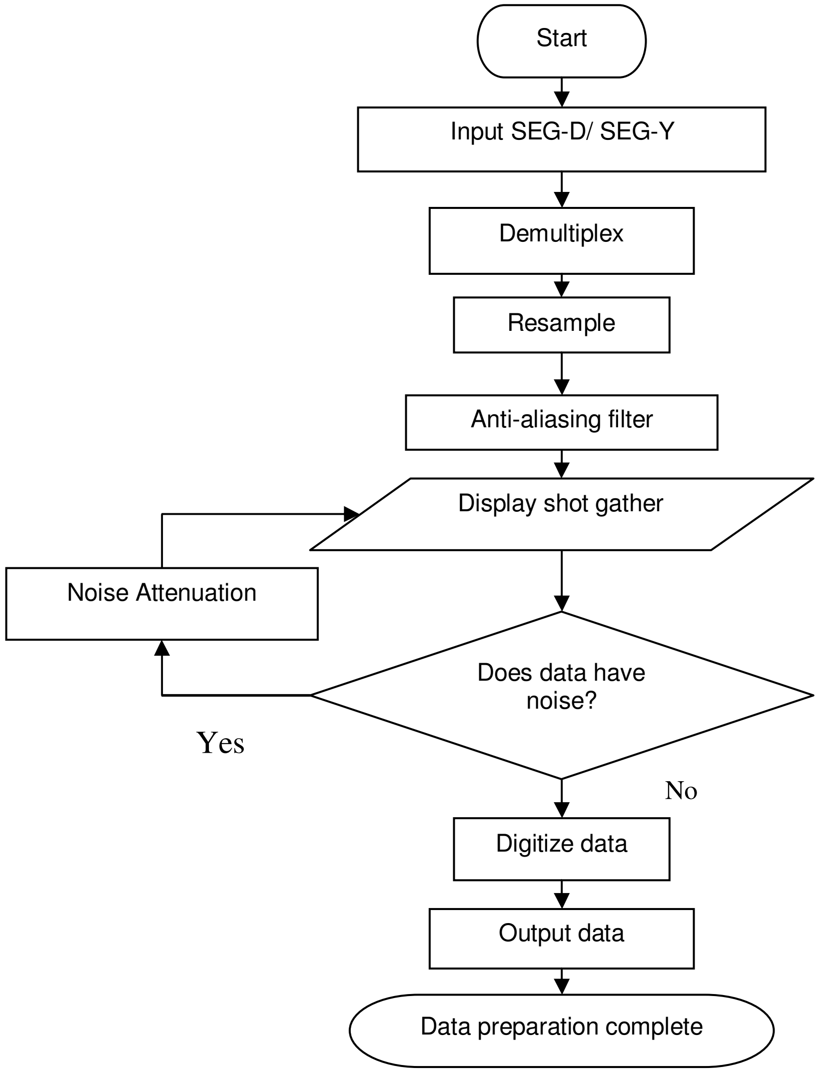

Figure1. Data preparation for amplitude matching and simulation

$s_{r1}t_{r11}a_{r11}$, s_{r1} is the first signal in the reversed shooting, t_{r11} is the first sampled time of the first signal in the reversed shooting, a_{r11} is the first sampled amplitude of the first signal in the reversed shooting. From the element, $s_{fL}t_{fLN}a_{fLN}$ in Figure 3, s_{fL} indicates the last signal in the forward shooting direction, t_{fLN} is the last sampled time of the last signal in the forward shooting direction, and a_{fLN} is the last sampled amplitude of the last signal in the forward shooting direction, and so on.

Scatter diagrams of the absolute amplitudes of the digitized seismic signals were plotted against the reflection time to assess the amplitude variation with time. When background noise and all other contaminated noise have been removed, the matching procedure can be started, after the maximum amplitude is identified.

The proposition is that, if the modulation index, Equation (1), can be increased, then the recorded seismic signal amplitude can also be increased. In other to increase the modulation index without any distortions in the seismic signal, the amplitudes at the later sample points ($a_0, a_1, a_2, \ldots, a_{N-1}$) are matched to the amplitude at the zero offset (a_0). If the amplitude at the zero offset is not measurable, matching can be done to the acceptable maximum amplitude (a_m) closest to the source position. This is because, the amplitude at the zero offset is equivalent to the maximum energy applied at the source position during acquisition. The computational procedure is illustrated below:

Assume that for one-dimensional (1D) seismic data (S_0), the un-scaled seismic amplitudes, $\{a_n\}$, on the recorded seismic signal with sample points (n) are given as:

$$S_0 = \{a_n\} = \{a_0, a_1, a_2, a_3, \ldots, a_{N-1}\}$$

(2)

To compute the first amplitude scaling function (S_1), we need to match the set of amplitudes in Equation (2) with the maximum amplitude, a_m, as explained above:

Detector(D):	*SP*	D_1	D_2	.	.	.	D_L
Offset(X):	*SP*	X_1	X_2	.	.	.	X_L
Signal(S):	*SP*	S_1	S_2	.	.	.	S_L

(a) End spread shooting geometry

$$\begin{bmatrix} s_1t_{11}a_{11} & s_2t_{21}a_{21} & . \; . \; . & s_Lt_{L1}a_{L1} \\ s_1t_{12}a_{12} & s_2t_{22}a_{22} & . \; . \; . & s_Lt_{L2}a_{L2} \\ s_1t_{13}a_{13} & s_2t_{23}a_{23} & . \; . \; . & s_Lt_{L3}a_{L3} \\ . & . & . \; . \; . & . \\ . & . & . \; . \; . & . \\ . & . & . \; . \; . & . \\ s_1t_{1N}a_{1N} & s_2t_{2N}a_{2N} & . \; . \; . & s_Lt_{LN}a_{LN} \end{bmatrix} \cong \begin{bmatrix} x_1t_{11}a_{11} & x_2t_{21}a_{21} & . \; . \; . & x_Lt_{L1}a_{L1} \\ x_1t_{12}a_{12} & x_2t_{22}a_{22} & . \; . \; . & x_Lt_{L2}a_{L2} \\ x_1t_{13}a_{13} & x_2t_{23}a_{23} & . \; . \; . & x_Lt_{L3}a_{L3} \\ . & . & . \; . \; . & . \\ . & . & . \; . \; . & . \\ . & . & . \; . \; . & . \\ x_1t_{1N}a_{1N} & x_2t_{2N}a_{2N} & . \; . \; . & x_Lt_{LN}a_{LN} \end{bmatrix}$$

(b) End spread matrix of sampled data of a shot gather.

Figure2. End-spread seismic acquisition geometry and sampled matrix array.

Detector (D):	D_{rL}	…	D_{r2}	D_{r1}	*SP*	D_{f1}	D_{f2}	…	D_{fL}
Offset (X):	X_{rL}	…	X_{r2}	X_{r1}	*SP*	X_{f1}	X_{f2}	…	X_{fL}
Signal (S):	S_{rL}	…	S_{r2}	S_{r1}	*SP*	S_{f1}	Sf_2	…	S_{fL}

(a) Split spread shooting geometry

$$\begin{bmatrix} s_{rL}t_{rL1}a_{rL1} & . \; . & s_{r2}t_{r21}a_{r21} & s_{r1}t_{r11}a_{r11} & s_{f1}t_{f11}a_{f11} & s_{f2}t_{f21}a_{f21} & . \; . & s_{fL}t_{fL1}a_{fL1} \\ s_{rL}t_{rL2}a_{rL2} & . \; . & s_{r2}t_{r22}a_{r22} & s_{r1}t_{r12}a_{r12} & s_{f1}t_{f12}a_{f12} & s_{f2}t_{f22}a_{f22} & . \; . & s_{fL}t_{fL2}a_{fL2} \\ s_{rL}t_{rL3}a_{rL3} & . \; . & s_{r2}t_{r23}a_{r23} & s_{r1}t_{r13}a_{r13} & s_{f1}t_{f13}a_{f13} & s_{f2}t_{f23}a_{f23} & . \; . & s_{fL}t_{fL3}a_{fL3} \\ . & . \; . & . & . & . & . & . \; . & . \\ . & . \; . & . & . & . & . & . \; . & . \\ s_{rL}t_{rLN}a_{rLN} & . \; . & s_{r2}t_{r2N}a_{r2N} & s_{r1}t_{r1N}a_{r1N} & s_{f1}t_{f1N}a_{f1N} & s_{f2}t_{f2N}a_{f2N} & . \; . & s_{fL}t_{fLN}a_{fLN} \end{bmatrix}$$

(b) Split spread matrix of sampled data of a shot gather.

Figure3. Split-spread seismic acquisition geometry and sampled matrix array

$$S_1 = \left\{ \frac{1}{2}(a_m + a_0), \frac{1}{2}(a_m + a_1), \frac{1}{2}(a_m + a_2), \ldots, \frac{1}{2}(a_m + a_{N-1}) \right\}$$
(3)

The second scaling function, S_2, is computed by matching the maximum amplitude, a_m, with those computed for S_1, as in Equation (3):

$$S_2 = \left\{ \frac{1}{2}\left[a_m + \frac{1}{2}(a_m + a_0)\right], \frac{1}{2}\left[a_m + \frac{1}{2}(a_m + a_1)\right], \frac{1}{2}\left[a_m + \frac{1}{2}(a_m + a_2)\right], \ldots, \frac{1}{2}\left[a_m + \frac{1}{2}(a_m + a_{N-1})\right] \right\}$$
(4)

Matching the amplitudes of S_2 with the maximum amplitude, a_m, the scaling function for S_3 can also be computed in a similar way. The set of sample amplitudes

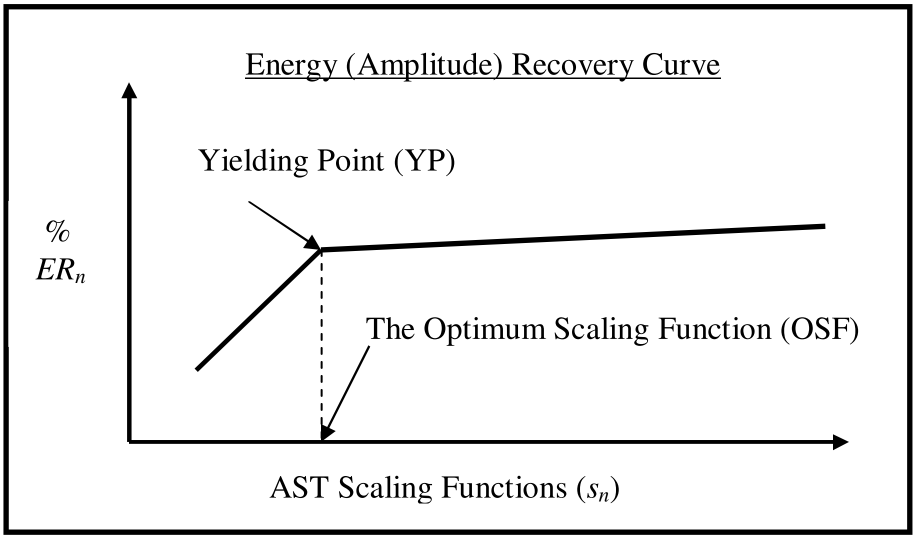

Figure4. ERC (or ARC) using AST scaling functions

computed using this concept give rise to a general sequence equation of the form:

$$S_{n+1} = \frac{a_m}{2}\left(1+\frac{\{s_n\}}{a_m}\right), \quad \text{where } n = 0, 1, 2 \ldots$$

(5)

If $n = 0$, Equation (5) can be written as:

$$S_1 = \frac{a_m}{2}\left(1+\frac{\{s_0\}}{a_m}\right)$$

$$= \frac{a_m}{2}\left(1+\frac{\{a_n\}}{a_m}\right) \quad \text{where } n = 0, 1, 2, \ldots, N\text{-}1$$

(6)

The ratio a_n/a_m is the modulation index (m_{id}) for each of the n^{th} sample points as indicated in Equation (1). Equation (6) is the general amplitude simulation function for any seismic data which needs energy or amplitude restoration. This concept can also be extended to multidimensional seismic signals by the addition of any chosen independent variable. For 2D seismic data, (t, y) or (f, k_y) and 3D, (t, y, z) or (f, k_y, k_z) seismic data, the equation for the scaling function can be expressed respectively as:

$$S_{n+1}(f,k_y) = \frac{a_m(f,k_y)}{2}\left(1+\frac{\{s_n(f,k)\}}{a_m(f,k_y)}\right) \quad (7)$$

$$S_{n+1}(f,k_y,k_z) = \frac{a_m(f,k_y,k_z)}{2}\left(1+\frac{\{s_n(f,k_y,k_z)\}}{a_m(f,k_y,k_z)}\right) \quad (8)$$

This process can be repeated iteratively until there is no or very little change in the result between S_n and S_{n+1}. The computation of m_{id}, is an important factor in this processing technique as, it is the factor that determines the strength and quality of the processed transmitted seismic signal, especially in frequency and wave-number domain.

In doing this, the initial energy or maximum amplitude will be distributed to sample points farther along the signal (or offsets) to restore the energy lost. This procedure can be repeated, for the trace, narrowing down the amplitude range between the source position, and the sample points farther from the source by half, each time, until all the amplitudes on the signal/trace are the same. The number of matching sets of modulation indexes we compute in the process is therefore equivalent to the number of possible sets of amplitude compensation scaling functions needed to restore the energy of the seismic signal.

Using Parseval's relations (Spiegel and Pettitt, 1983; Stroud and Booth, 2003), the signal energy (E_n) and the power (P_n) of all the computed scaling functions can be estimated. If the computed energy or power of the initial seismic signal is E_0 or P_0, the percentage energy (amplitude) recovery (% ER_n) or power recovery (% PR_n) of the computed AST scaling functions (k) can be expressed respectively as:

$$\%ER_n = \left(1-\frac{E_0}{\sum_{n=0}^{k}|s_n|^2}\right) \text{ x } 100 \quad \text{or}$$

$$\%PR_n = \left(1-\frac{P_0}{\frac{1}{N}\sum_{n=0}^{k}|s_n|^2}\right) \text{ x } 100 \text{ for } n = 0, 1, 2, \ldots, k$$

(9)

RESULTS AND DISCUSSIONS

To find a suitable scaling function, in order to compensate for the lost of energy (or amplitudes) at farther samples, and still maintaining the integrity of the seismic signal signatures, a graph of the percentage energy (amplitude) recovery (ERC or ARC), versus the computed scaling functions can be constructed, using Equation (9).

As shown in Figure (4) above, the Optimum Scaling Function (OSF) to compensate for the lost of energy in the seismic signal is the scaling function at the yielding point (YP). Any of the AST scaling functions beyond this point, will show a much better seismic section than when any of the conventional scaling functions is applied. The signal signature of the formations in the subsurface would also be preserved with the use of the AST scaling function than with the conventional scaling methods. However, the farther the chosen AST scaling functions is from the yielding point (YP), the closer it approaches a conventional scaling function, and the more flatter the amplitudes become.

CONCLUSION

The application of the optimum scaling function (OSF), from the percentage energy recovery curve, to the seismic data, retained the signal signature, unlike the conventional scaling functions, which provide a scalar value to flatten all the amplitudes, and then destroy the seismic signatures. With the AST scaling functions, the final seismic section have improved signal-to-noise ratio compared to the conventional scaling methods. Structures which were not possible to identify on the seismic sections when processed with conventional scaling methods are easily delineated when the AST scaling functions are used in the pre-stack processing stage of the seismic processing steps.

ACKNOWLEDGMENTS

The following members of the academia were of tremendous help to this work. First and foremost, we would like to thank Professor Daniel K. Asiedu, Professor D. Atta-Peters, Professor P. M. Nude, and Dr. Thomas Armah, all of Department of Earth Science in the University of Ghana. We are particularly grateful to Mr Emmanuel Asiedu Akyeampong of the Balme Library of the University of Ghana, who helped in the editing of this work. Special mention is also made to both workers at the Ghana National Petroleum Corporation (GNPC) and the Department of Earth Science, University of Ghana, for their permission to use their facilities.

REFERENCES

Claerbout JF (1976). Fundamentals of geophysical data processing. McGraw-Hill. ISBN 1-56080-137-9.

Dobrin MB, Savit CH (1988). Introduction to Geophysical Prospecting, McGraw-Hill Book Co., New York, USA.

Frank AJR (1974), Theory and Problems of Matrices, SI (metric) edition, Schaum's Outline Series, McGraw-Hill, USA.

Gupta JB (2009). Electronic Devices and Circuits, Third Edition, New Delhi, India: SK Kataria and Sons.

Henry G (1997). Geophysics for Sedimentary Basins, Editions Technip, Paris, France, Pp1 – 445.

Ikelle LT, Lasse A (2005). Introduction to Petroleum Seismology. Society of Exploration Geophysicists. ISBN 1-56080-129-8.

Kearey P, Brooks M (2002). An Introduction to Geophysical Exploration, Blackwell, UK.

Mike H (2007). Marine seismic surveys with enhanced azimuth coverage: Lessons in survey design and acquisition (PDF). The Leading Edge (SEG) **26** (4): 480. (Retrieved September 8, 2013).

Palmer D (1980). The generalized reciprocal method of seismic refraction interpretation: Soc. Expl. Geophys. Pp104

Sandmeier KJ (2012). REFLEXW (Software), Version 7.0, Germany: Karisruhe.

Sheriff RE (1991), Encyclopedic dictionary of exploration geophysics, Third Edition, Society of Exploration Geophysicists, Tulsa, USA. Pp 1 – 376.

Spiegel MR, Pettitt AN (1983). Advanced Mathematics for Engineers and Scientists, Schaum's Outline Series, McGraw-Hill, Singapore.

Stroud KA, Booth DJ (2003), Advanced Engineering Mathematics, Fourth Edition, Palgrave Macmillan Ltd, UK.

Telford WM, Geldart LP, Sheriff RE (1990). Applied Geophysics, Second Edition, Cambridge University Press, Cambridge, UK.

Western Geophysical Division (1998). Seismic Data Processing Concepts 1&II, Western Atlas International Inc., London, UK.

Yilmaz OZ (2001). Seismic data analysis. Society of Exploration Geophysicists. ISBN 1-56080-094-1.

How to cite this article: Oppong I.A. and Danour S.K. (2014). Amplitude Simulation Technique for Seismic Amplitude Scaling. Int. Res. J. Geo. Min. 4(5): 133-138